Fast Maximum-Likelihood Decoding of the Golden Code

Mohanned O. Sinnokrot, *Student Member, IEEE,* and John R. Barry, *Senior Member, IEEE*

***Abstract*—Because each golden code codeword conveys four information symbols from an M-ary QAM alphabet, the complexity of an exhaustive-search decoder is proportional to M^4. In this paper we prove that the golden code is *fast-decodable*, meaning that maximum-likelihood decoding is possible with a worst-case complexity proportional to only $M^{2.5}$. The golden code retains its fast-decodable property regardless of whether the channel varies with time. We also present an efficient implementation of a fast maximum-likelihood decoder that exhibits a low average complexity.**

***Index Terms*—Golden code, maximum-likelihood decoding.**

I. Introduction

SPACE-time coding enables a wireless transmitter with more than one antenna to communicate at a higher data rate and more reliably than would otherwise be possible [1][2]. The golden code is a space-time code for two transmit and two or more receive antennas that has many advantages [3][4]: it is full-rate; it is fully diverse; and in terms of the signal-to-noise ratio (SNR) required to achieve a target error probability, it performs better than previously reported codes with two transmit antennas. Furthermore, the coding gain of the golden code is independent of the alphabet size, which ensures that the golden code achieves the full diversity-multiplexing frontier of Zheng and Tse [5][6], and which makes it compatible with adaptive modulation. For these reasons, the golden code has been incorporated into the 802.16e WiMAX standard [7].

The golden code applied to a system with two receive antennas leads to an *effective* four-input four-output channel that maps each block of four M-ary information symbols to a vector of four complex-valued received samples [8]. An exhaustive-search maximum-likelihood (ML) decoder would consider each of the M^4 possible input vectors in turn and choose as its decision the one that best represents the channel output in a minimum-distance sense. Therefore, the complexity of such an ML decoder is proportional to M^4. Although significant reductions in *average* complexity are possible by adopting a tree-based ML decoder such as a sphere decoder, the *worst-case* complexity of a sphere decoder is generally no better than that of an exhaustive-search. For this reason, it has been reported that the worst-case complexity of the golden code grows with the fourth power of the constellation size [9]-[12]. In the special case when the four inputs are QAM symbols, however, the worst-case complexity of a tree-based sphere decoder drops from $\mathcal{O}(M^4)$ to $\mathcal{O}(M^3)$. This is because a QAM slicer can be used to find the "best" leaf node stemming from a particular node at the third level of the four-level tree, and the complexity of a QAM slicer does not grow with the size of the alphabet.[1]

The perception that ML decoding of the golden code has high complexity has had two effects: First, it has motivated a search for suboptimal decoders for the golden code with reduced complexity and near-ML performance [13]-[16]. Second, it has motivated a search for lower-complexity alternatives that perform almost as well as the golden code [9][10][17].

In this paper we prove that the golden code with M-ary QAM is *fast decodable*, by which we mean that ML decoding is possible with a worst-case complexity of only $\mathcal{O}(M^{2.5})$. The golden code is fast decodable regardless of whether the channel varies with time. We also present an efficient implementation of a fast decoder that has low average complexity. For concreteness we present our results in the context of the Dayal-Varanasi golden code [4], but they are in fact applicable to all three variations [3][4][7].

The remainder of the paper is organized as follows. In Section II, we review the construction of the golden code and prove that it is fast decodable. In Section III we introduce a new fast ML decoder for the golden code that has low average complexity. In Section IV, we compare the average complexity of the proposed detector to a conventional golden code detector. We conclude the paper in Section V.

II. The Golden Code is Fast Decodable

A. The Golden Code Induces Structure in Effective Channel

The golden code transmits four complex information symbols over two symbol periods, so that the rate is two symbols per signaling interval. The transmitted codeword can be expressed as

$$\mathbf{C} = \begin{bmatrix} c_1[1] & c_2[1] \\ c_1[2] & c_2[2] \end{bmatrix}, \qquad (1)$$

where $c_i[k]$ denotes the symbol transmitted from antenna $i \in \{1, 2\}$ at time $k \in \{1, 2\}$. In particular, the Dayal-Varanasi golden code encodes one pair of information symbols $\mathbf{a} = [x_1, x_2]^\top$ onto the main diagonal of $\mathbf{C}$, and it encodes a second pair of symbols $\mathbf{b} = [x_3, x_4]^\top$ onto the off-diagonal, yielding [4]:

$$\mathbf{C} = \begin{bmatrix} \tilde{a}_1 & 0 \\ 0 & \tilde{a}_2 \end{bmatrix} + \phi \begin{bmatrix} 0 & \tilde{b}_1 \\ \tilde{b}_2 & 0 \end{bmatrix} \qquad (2)$$

[1] A QAM slicer can be implemented as a pair of PAM slicers, with each requiring a single multiply, a single rounding operation, a single addition, and a single hard-limiting operation, none of which depends on M.

Manuscript received November 12, 2008; revised April 22, 2009; accepted July 16, 2009. The associate editor coordinating the review of this letter and approving it for publication was M. Uysal.

M. O. Sinnokrot and J. R. Barry are with the Department of Electrical and Computer Engineering, Georgia Institute of Technology, Atlanta, GA, 30332 USA (e-mail: {sinnokrot, barry}@ece.gatech.edu).

This work was supported in part by a grant from Texas Instruments. The material in this correspondence was presented at the IEEE Global Communications Conference, New Orleans, LA, USA, December 2008.

Digital Object Identifier 10.1109/TWC.2010.01.081512

1536-1276/10$25.00 © 2010 IEEE

where:

$$\tilde{\mathbf{a}} = \mathbf{M}\mathbf{a}, \quad \tilde{\mathbf{b}} = \mathbf{M}\mathbf{b}, \quad \mathbf{M} = \begin{bmatrix} \cos(\theta) & \sin(\theta) \\ -\sin(\theta) & \cos(\theta) \end{bmatrix},$$
$$\theta = \frac{1}{2}\tan^{-1}(2), \quad \phi = e^{j\pi/4}. \tag{3}$$

Our model for the received signal $y_j[k]$ at receive antenna j at time k is given by:

$$y_j[k] = \sum_{i=1}^{2} c_i[k] h_{i,j}[k] + n_j[k], \tag{4}$$

where $n_j[k]$ is the complex additive-white Gaussian noise at receive antenna j at time k, and $h_{i,j}[k]$ is the channel coefficient between the i-th transmit antenna and j-th receive antenna at time k. For quasistatic fading, $h_{i,j}[k] = h_{i,j}$ is independent of time k. Substituting the definition of the golden code from (2) and (3) into (4), the vector of samples $\mathbf{y} = [y_1[1], y_1[2], y_2[1], y_2[2]]^\top$ received at a receiver with two antennas at the two time instances can be written as the output of an effective four-input four-output channel:

$$\mathbf{y} = \mathbf{H}\mathbf{x} + \mathbf{n}, \tag{5}$$

where $\mathbf{x} = [x_1, x_2, x_3, x_4]^\top$ is the vector of information symbols, $n = [n_1[1], \ldots, n_2[2]]^\top$ is the noise, and where $\mathbf{H} = \bar{\mathbf{H}}\Psi$ is the *effective channel matrix*:

$$\mathbf{H} = \underbrace{\begin{bmatrix} h_{1,1}[1] & 0 & \phi h_{2,1}[1] & 0 \\ 0 & h_{2,1}[2] & 0 & \phi h_{1,1}[2] \\ h_{1,2}[1] & 0 & \phi h_{2,2}[1] & 0 \\ 0 & h_{2,2}[2] & 0 & \phi h_{1,2}[2] \end{bmatrix}}_{\bar{\mathbf{H}}} \underbrace{\begin{bmatrix} c & s & 0 & 0 \\ -s & c & 0 & 0 \\ 0 & 0 & c & s \\ 0 & 0 & -s & c \end{bmatrix}}_{\Psi}, \tag{6}$$

where $c = \cos(\theta)$, $s = \sin(\theta)$, $\phi = e^{j\pi/4}$, and $\theta = \frac{1}{2}\tan^{-1}(2)$.

The structure of the golden code induces special properties in this effective matrix that we exploit to reduce decoding complexity. The following lemma relates these special properties to the orthogonal-triangular (QR) decomposition $\mathbf{H} = \mathbf{QR}$, which results from an application of the Gram-Schmidt procedure to the columns of $\mathbf{H} = [\mathbf{h}_1, \ldots, \mathbf{h}_4]$, where $\mathbf{Q} = [\mathbf{q}_1, \ldots, \mathbf{q}_4]$ is unitary and $\mathbf{R}$ is upper triangular with nonnegative real diagonal elements, so that the entry of $\mathbf{R}$ in row i and column j is $r_{i,j} = \mathbf{q}_i^* \mathbf{h}_j$.

Lemma 1: (*The Key Property*): The $\mathbf{R}$ matrix in a QR decomposition $\mathbf{H} = \mathbf{QR}$ of the effective channel (6) has the form

$$\mathbf{R} = \begin{bmatrix} \mathbf{A} & \mathbf{B} \\ \mathbf{0} & \mathbf{D} \end{bmatrix}, \tag{7}$$

where both of the upper triangular matrices $\mathbf{A}$ and $\mathbf{D}$ are entirely real.

Proof: See the Appendix. ■

A few remarks:

- Both $\mathbf{A} = \begin{bmatrix} r_{1,1} & r_{1,2} \\ 0 & r_{2,2} \end{bmatrix}$ and $\mathbf{D} = \begin{bmatrix} r_{3,3} & r_{3,4} \\ 0 & r_{4,4} \end{bmatrix}$ are triangular by construction with real diagonal entries, so the key property is essentially the fact that both $r_{1,2}$ and $r_{3,4}$ are real.
- To demonstrate that $r_{1,2} = \mathbf{h}_1^* \mathbf{h}_2 / \|\mathbf{h}_1\|$ is real, it is sufficient to show that the inner product between the first two columns is real, a fact which is easily verified by direct computation:

$$\begin{aligned} \mathbf{h}_1^* \mathbf{h}_2 &= \cos(\theta)\sin(\theta)(|h_{1,1}[1]|^2 - |h_{2,1}[2]|^2 + \\ &\quad |h_{1,2}[1]|^2 - |h_{2,2}[2]|^2) \\ &= \frac{1}{\sqrt{5}}(|h_{1,1}[1]|^2 - |h_{2,1}[2]|^2 + \\ &\quad |h_{1,2}[1]|^2 - |h_{2,2}[2]|^2). \end{aligned} \tag{8}$$

- The lemma applies regardless of whether the channel is quasistatic or time-varying.
- The submatrix $\mathbf{B}$ is not mentioned because all four of its entries are generally complex.
- The fact that $r_{1,2}$ is real enables the decoder in the next section to reduce both the worst-case decoding complexity and the average decoding complexity. In contrast, the fact that $r_{3,4}$ is real enables only a reduction in average complexity. It has no impact on the worst-case complexity.

B. The Golden Code is Fast Decodable

We now show how the key property of Lemma 1 enables fast decoding. If we define $\mathbf{z}_{12} = [z_1, z_2]^\top$ and $\mathbf{z}_{34} = [z_3, z_4]^\top$, where $\mathbf{z} = \mathbf{Q}^*\mathbf{y}$, then the ML decision minimizes the cost function

$$\begin{aligned} P(\mathbf{x}) &= \|\mathbf{y} - \mathbf{Hx}\|^2 = \|\mathbf{z} - \mathbf{Rx}\|^2 \\ &= \|\mathbf{z}_{12} - \mathbf{Aa} - \mathbf{Bb}\|^2 + \|\mathbf{z}_{34} - \mathbf{Db}\|^2. \end{aligned} \tag{9}$$

The last equality follows from (7). Therefore, the ML decisions $\hat{\mathbf{a}}$ and $\hat{\mathbf{b}}$ can be found recursively using:

$$\hat{\mathbf{b}} = \arg\min_{\mathbf{b} \in \mathcal{A}^2} \{\|\mathbf{z}_{12} - \mathbf{A}\mathbf{a}_*(\mathbf{b}) - \mathbf{Bb}\|^2 + \|\mathbf{z}_{34} - \mathbf{Db}\|^2\}, \tag{10}$$

$$\hat{\mathbf{a}} = \mathbf{a}_*(\hat{\mathbf{b}}), \tag{11}$$

where

$$\mathbf{a}_*(\mathbf{b}) = \arg\min_{\mathbf{a} \in \mathcal{A}^2} \{\|\mathbf{z}_{12} - \mathbf{Aa} - \mathbf{Bb}\|^2\}. \tag{12}$$

The function $\mathbf{a}_*(\mathbf{b})$ in (12) can be viewed as producing the best $\mathbf{a}$ for a given $\mathbf{b}$. With this interpretation, the optimization in (10) can be viewed as that of finding the best $\mathbf{b}$ when $\mathbf{a}$ is optimized.

The optimization (12) is equivalent to ML detection for a channel matrix $\mathbf{A}$ with an input of $\mathbf{a}$ and an output:

$$\mathbf{v} = \mathbf{z}_{12} - \mathbf{Bb}. \tag{13}$$

It can thus be solved by a sphere detector applied to a two-level tree. As discussed in the introduction, with two QAM inputs and without any constraints on $\mathbf{A}$, its worst-case complexity would be $\mathcal{O}(M)$. But the golden code induces the special property that $\mathbf{A}$ is real, which enables us to determine the real components of $\mathbf{a}$ *independently* from its imaginary components in (12). Specifically, we may rewrite (12) as:[2]

$$\begin{aligned}\mathbf{a}_*(\mathbf{b}) &= \arg\min_{\mathbf{a}\in\mathcal{A}^2}\{\|\mathbf{v}^R-\mathbf{A}\mathbf{a}^R\|^2 + \\ &\quad \|\mathbf{v}^I-\mathbf{A}\mathbf{a}^I\|^2\} \qquad (14)\\ &= \arg\min_{\mathbf{a}^R\in(\mathcal{A}^R)^2}\{\|\mathbf{v}^R-\mathbf{A}\mathbf{a}^R\|^2\} + \\ &\quad j\cdot\arg\min_{\mathbf{a}^I\in(\mathcal{A}^I)^2}\{\|\mathbf{v}^I-\mathbf{A}\mathbf{a}^I\|^2\}. \qquad (15)\end{aligned}$$

Thus, the optimization in (12) decomposes into the pair of independent optimizations of (15). Since each optimization in (15) is equivalent to ML detection for a real channel with two $\sqrt{M}$-PAM inputs, each has a worst-case complexity of $\mathcal{O}(\sqrt{M})$. Thus, the overall complexity of (15) is $\mathcal{O}(\sqrt{M})$. We thus arrive at our main theorem.

Theorem 1: (*Golden Code is Fast Decodable*): A maximum-likelihood decoder for the golden code with an M-ary QAM alphabet can be implemented with a worst-case complexity of $\mathcal{O}(M^{2.5})$.

Proof: As described in (10), the ML decision can be found by stepping through each of the M^2 candidate values for $\mathbf{b}$, and for each implement the $\mathcal{O}(\sqrt{M})$ optimization of (15). ■

III. A Fast ML Decoder With Low Average Complexity

The decoding strategy used to prove the fast-decodable theorem has a low worst-case complexity but a high average complexity. In this section we present an efficient implementation of an ML decoder for the golden code that has both low average complexity and a worst-case complexity of $\mathcal{O}(M^{2.5})$.

A conventional sphere decoder for the golden code is based on a four-level tree, with a different x_i associated with each level. In contrast, as illustrated in Fig. 1, we propose a four-level tree that associates $\mathbf{b}^R = (x_3^R, x_4^R)$ with the first level, $\mathbf{b}^I = (x_3^I, x_4^I)$ with the second level, $\mathbf{a}^R = (x_1^R, x_2^R)$ with the third level, and $\mathbf{a}^I = (x_1^I, x_2^I)$ with the fourth level. This new tree is a direct result of the fact that $\mathbf{A}$ and $\mathbf{D}$ are real (Lemma 1), which allows us to rewrite the ML cost function from (9) as

$$\begin{aligned}P(\mathbf{x}) &= \underbrace{\|\mathbf{v}^I-\mathbf{A}\mathbf{a}^I\|^2}_{P_1} + \underbrace{\|\mathbf{v}^R-\mathbf{A}\mathbf{a}^R\|^2}_{P_2} + \\ &\quad \underbrace{\|\mathbf{z}_{34}^I-\mathbf{D}\mathbf{b}^I\|^2}_{P_3} + \underbrace{\|\mathbf{z}_{34}^R-\mathbf{D}\mathbf{b}^R\|^2}_{P_4}. \qquad (16)\end{aligned}$$

Thus, as illustrated in Fig. 1, (16) shows that the total cost of a leaf node $\mathbf{x}$ decomposes into the sum $\sum_i P_i$ of four branch metrics, where P_i denotes the branch metric for a branch at the $(4-i)$-th stage of the tree.

Besides inducing a new tree structure, the fact that $\mathbf{D}$ is real also leads to a significant reduction in the complexity of the Schnorr-Euchner sorting for the first two stages of the tree. Specifically, the fact that $\mathbf{D}$ is real leads to a second-stage branch metric P_3 that is *independent* of the starting node ($\mathbf{b}^R$). Therefore, we can perform a single sort for the symbol pair ($\mathbf{b}^R$) emanating from the root, and *simultaneously* a single sort for the symbol pair ($\mathbf{b}^I$) emanating from its children.

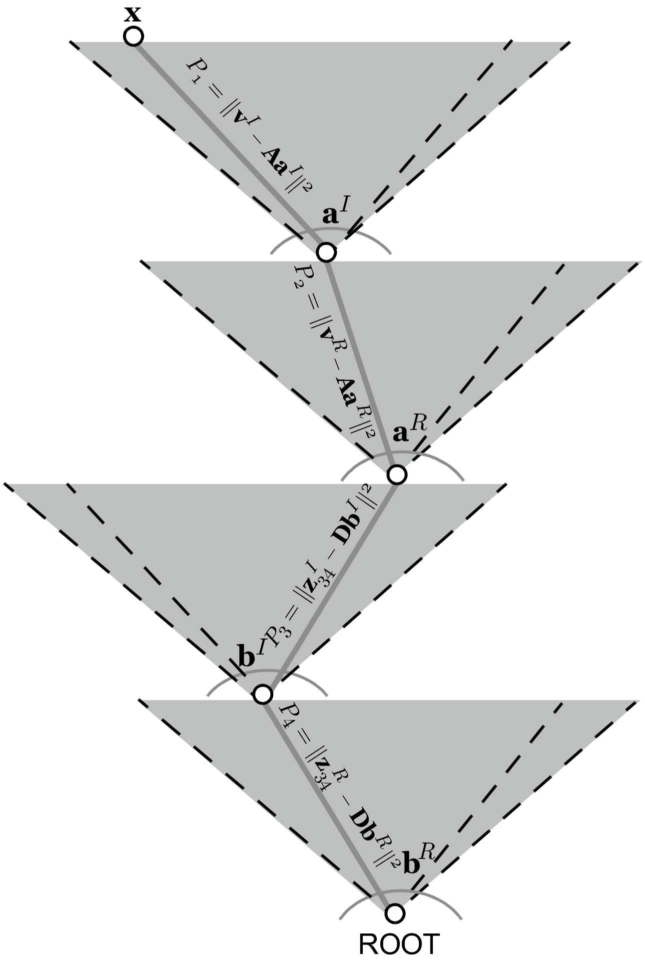

x
$P_1 = \|\mathbf{v}^I - \mathbf{A}\mathbf{a}^I\|^2$
$\mathbf{a}^I$
$P_2 = \|\mathbf{v}^R - \mathbf{A}\mathbf{a}^R\|^2$
$\mathbf{a}^R$
$P_3 = \|\mathbf{z}_{34}^I - \mathbf{D}\mathbf{b}^I\|^2$
$\mathbf{b}^I$
$P_4 = \|\mathbf{z}_{34}^R - \mathbf{D}\mathbf{b}^R\|^2$
$\mathbf{b}^R$
ROOT

Fig. 1. The structure of the proposed detection tree and its branch metrics. The cost function for the leaf node is the sum of the branch metrics, $P(\mathbf{x}) = P_1 + P_2 + P_3 + P_4$.

The pseudocode of an efficient implementation of the proposed ML golden code detector is shown in Fig. 2. The first five lines represent initializations. In particular, the first two lines are a QR decomposition of the effective channel matrix in (6) and the computation of $\mathbf{z}$ in (9). The squared sphere radius $\hat{P}$, which represents the smallest cost (16) encountered so far, is initialized to infinity to ensure ML decoding (line 3). Sorting or Schnorr-Euchner enumeration is used for faster convergence. Only two sorting operations (line 4 and line 5) are required. In the pseudocode, the complex QAM alphabet $\mathcal{A}$ is represented by an ordered list, so that $\mathcal{A}(k)$ indexes the k-th symbol in the list.

The remainder of algorithm can be interpreted as a two-level *complex* sphere decoder to choose the symbol pair $\mathbf{b} = (x_3, x_4)^\top$, followed by an independent pair of two-level *real* sphere decoders that separately decode $\mathbf{a}^R = (x_1^R, x_2^R)^\top$ and $\mathbf{a}^I = (x_1^I, x_2^I)^\top$.

The two-level complex sphere decoder incorporates two common optimizations: radius update (line 47) and pruning (line 7, line 11). While these optimizations do not affect the worst-case complexity, they affect the average complexity significantly. The first level of the complex sphere decoder considers candidate pairs $\mathbf{b}^R$ in ascending order of their branch metric P_4 (line 6). The second level of the complex

[2] Throughout the paper we use superscripts R and I to denote the real and imaginary components, respectively, so that $v^R = \Re\{v\}$ and $a^I = \Im\{a\}$.

```
1  $[\mathbf{Q}, \mathbf{R}] =$ QR decomposition($\mathbf{H}$)
2  $\mathbf{z} = \mathbf{Q}^*\mathbf{y}$
3  $\hat{P} = \infty$
4  $[P_4, \Pi_4] =$
   $\texttt{sort}_{a\in\mathcal{A}}((z_3^R - r_{3,3}a^R - r_{3,4}a^I)^2 + (z_4^R - r_{4,4}a^I)^2)$
5  $[P_3, \Pi_3] =$
   $\texttt{sort}_{a\in\mathcal{A}}((z_3^I - r_{3,3}a^R - r_{3,4}a^I)^2 + (z_4^I - r_{4,4}a^I)^2)$
6  for $k$ from 1 to $M$ do
7      if $(P_4(k) + P_3(1)) > \hat{P}$ then
8          break
9      end
10     for $l$ from 1 to $M$ do
11         if $(P_3(l) + P_4(k)) > \hat{P}$ then
12             break
13         end
14         $[x_3^R, x_3^I, x_4^R, x_4^I] =$
           $[\mathcal{A}(\Pi_4(k))^R, \mathcal{A}(\Pi_3(l))^R, \mathcal{A}(\Pi_4(k))^I, \mathcal{A}(\Pi_3(l))^I]$
15         $v_1 = z_1 - r_{1,3}x_3 - r_{1,4}x_4$
16         $v_2 = z_2 - r_{2,3}x_3 - r_{2,4}x_4$
17         $\hat{P}_1 = \hat{P}_2 = \hat{P}$
18         $\mathcal{X} = \texttt{list}(v_2^R / r_{2,2})$
19         for $m$ from 1 to $\sqrt{M}$ do
20             $P_2 = (v_2^R - r_{2,2}\mathcal{X}(m))^2$
21             if $P_2 > \hat{P}_2$ then
22                 break
23             end
24             $u_1^R = v_1^R - r_{1,2}\mathcal{X}(m)$
25             $q = Q(u_1^R / r_{1,1})$
26             $P_2 = (u_1^R - r_{1,1}q)^2 + P_2$
27             if $P_2 < \hat{P}_2$ then
28                 $x_1^R = q$, $x_2^R = \mathcal{X}(m)$, $\hat{P}_2 = P_2$
29             end
30         end
31         $\mathcal{X} = \texttt{list}(v_2^I / r_{2,2})$
32         for $n$ from 1 to $\sqrt{M}$ do
33             $P_1 = (v_2^I - r_{2,2}\mathcal{X}(n))^2$
34             if $P_1 > \hat{P}_1$ then
35                 break
36             end
37             $u_1^I = v_1^I - r_{1,2}\mathcal{X}(n)$
38             $q = Q(u_1^I / r_{1,1})$
39             $P_1 = (u_1^I - r_{1,1}q)^2 + P_1$
40             if $P_1 < \hat{P}_1$ then
41                 $x_1^I = q$, $x_2^I = \mathcal{X}(n)$, $\hat{P}_1 = P_1$
42             end
43         end
44         $P = \hat{P}_1 + \hat{P}_2 + P_3(l) + P_4(k)$
45         if $P < \hat{P}$ then
46             $\hat{\mathbf{x}} = [x_1, x_2, x_3, x_4]$
47             $\hat{P} = P$
48         end
49     end
50 end
```

Fig. 2. Pseudocode of a fast ML decoder for the golden code.

sphere decoder considers candidate pairs $\mathbf{b}^I$ in ascending order of their branch metric P_3 (line 10). After forming $\mathbf{b} = [x_3, x_4]^\top$ (line 14), the decoder removes the interference caused by $\mathbf{b}$ and forms the two intermediate variables v_1 and v_2 of (13), which are functions of the symbols x_1 and x_2 only (line 15 and line 16). Following the two-level complex sphere decoder and interference cancellation, the decoder decides on the symbol pairs $\mathbf{a}^R$ and $\mathbf{a}^I$ separately using an independent pair of two-level real sphere decoders.

The function `list` is used to implement sorting for the final two stages of the tree; it returns a list of candidate symbols drawn from the $\sqrt{M}$-ary PAM alphabet $\mathcal{A}^R$, sorted in ascending order of distance to the input argument. As described in [18], it can be implemented efficiently using a table lookup.

After initializing the sphere radius for decoding $\mathbf{a}^R = (x_1^R, x_2^R)^\top$ (line 17) and forming the sorted list of best candidate symbols (line 18), the real sphere decoder chooses the symbol x_2^R that has the lowest branch metric P_2 (line 20). The interference from the symbol x_2^R is then subtracted (line 24) and a decision is made on the symbol x_1^R using the PAM slicer $Q(\ \cdot\ )$ (line 25); the slicer function $Q(\ x\ )$ returns the symbol from the PAM alphabet $\mathcal{A}^R$ that is closest to x. The branch-metric P_2 for the current candidate symbol pair $\mathbf{a}^R$ is computed in line 26, and radius update occurs if it is less than the previous smallest value $\hat{P}_2$ (line 28). The real sphere decoder includes pruning and radius update (line 21 and line 28, respectively).

Decoding the symbol pair $\mathbf{a}^I$ follows identically to the decoding of the symbol pair $\mathbf{a}^R$ and is shown in line 31 through line 43. Importantly, $\mathbf{a}^R$ and $\mathbf{a}^I$ are decoded independently. Therefore, although the pseudocode shows a serial implementation that decodes first $\mathbf{a}^R$ and second $\mathbf{a}^I$, a hardware implementation could decode them simultaneously (in parallel), thus decreasing decoding latency. The overall cost P for the current candidate symbol vector is updated in line 44. Radius update and best candidate vector update occurs if the current cost P is less than the previous smallest cost $\hat{P}$ (line 46 and line 47, respectively).

The algorithm could be embellished to further reduce average complexity. For example, the columns of $\mathbf{H}$ could be permuted using a BLAST ordering. (In this case the only permutations for which the key property of Lemma 1 will still hold are $\{1, 2, 3, 4\}$, $\{1, 2, 4, 3\}$, $\{2, 1, 3, 4\}$, $\{2, 1, 4, 3\}$, $\{3, 4, 1, 2\}$, $\{3, 4, 2, 1\}$, $\{4, 3, 1, 2\}$ and $\{4, 3, 2, 1\}$.) For the sake of clarity of exposition, however, we have chosen not to include such refinements in Fig. 2. Such refinements, which have no effect on the worst-case complexity, are well-known in the literature and their application to the pseudocode is straightforward.

We remark that a quasistatic channel does not offer any additional reduction in decoding complexity, as compared to a time-varying channel. This is a direct result of the fact that the entries of $\mathbf{B}$ in (7) are generally complex, regardless of whether the channel is quasistatic or time-varying.

IV. Numerical Results

In Fig. 3 we compare the average complexity of the proposed fast ML decoder to a conventional ML decoder.

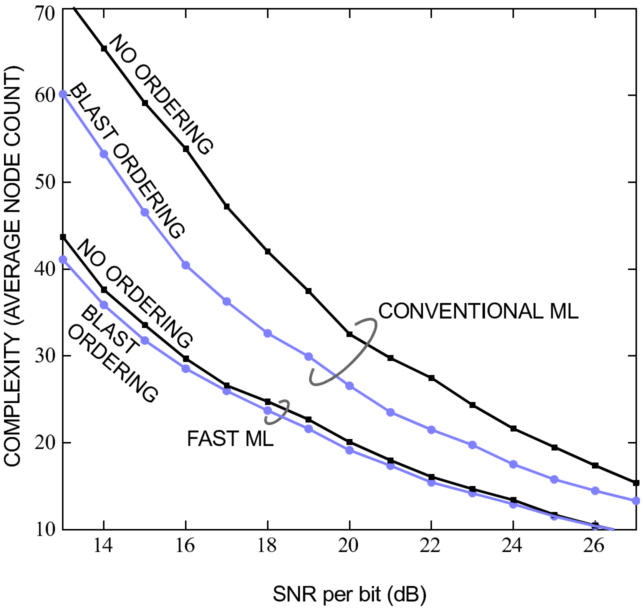

Fig. 3. Average decoding complexity versus SNR for golden code with 64-QAM.

The average complexity is quantified by the average number of nodes visited while searching the tree. The channel was modeled using (4) with quasistatic i.i.d. Rayleigh fading, with constant coefficients within each codeword block, but independent fading from block to block. The alphabet was 64-QAM. The fast ML decoder was implemented following the pseudocode of Fig. 2. The conventional ML decoder was implemented using an efficient four-level complex sphere decoder with Schnorr-Euchner enumeration. Results are shown for two cases of channel matrix column ordering: no ordering and BLAST reordering.

As can be seen from Fig. 3, with no column ordering, the proposed fast ML decoder is about 45% less complex than a conventional ML decoder. With BLAST ordering, the proposed ML decoder is about 30% less complex than a conventional decoder. Beyond the advantages shown in Fig. 3, the proposed algorithm has three additional advantages that are not reflected in Fig. 3, namely:

- the proposed algorithm reduces the number of Schnorr-Euchner sort operations for the first two stages to only two, compared with a conventional decoder that can require as many as $M+1$.
- the proposed algorithm can avoid BLAST ordering without a high complexity penalty.
- decoding of the symbol pairs $\mathbf{a}^R$ and $\mathbf{a}^I$ can be done in parallel, reducing decoding latency.

V. Conclusion

The golden code induces special structure in the effective channel matrix. By recognizing and exploiting this structure we have proven that the worst-case complexity of an ML decoder for the golden code with M-ary QAM is $\mathcal{O}(M^{2.5})$, regardless of whether the channel varies with time. By further exploiting this structure we have proposed a fast ML decoding algorithm based on a unique tree construction that outperforms a conventional ML detector on four fronts simultaneously: worst-case complexity, average complexity, sorting complexity, and decoding latency.

Appendix
Proof of The Key Property (Lemma 1)

We will use a QR decomposition of $\bar{\mathbf{H}}$ from (6), namely $\bar{\mathbf{H}} = \bar{\mathbf{Q}}\bar{\mathbf{R}}$, to construct a QR decomposition of $\mathbf{H} = \bar{\mathbf{H}}\Psi$, namely $\mathbf{H} = \mathbf{QR}$.

Inspection of (6) reveals that $\bar{\mathbf{h}}_1^*\mathbf{h}_2 = \bar{\mathbf{h}}_1^*\mathbf{h}_4 = \bar{\mathbf{h}}_2^*\mathbf{h}_3 = \bar{\mathbf{h}}_3^*\mathbf{h}_4 = 0$, which implies that the subspace spanned by the first and third columns of $\bar{\mathbf{H}}$ is orthogonal to the subspace spanned by the second and fourth columns. This fact implies that $\bar{r}_{1,2} = \bar{r}_{1,4} = \bar{r}_{2,3} = \bar{r}_{3,4} = 0$, so that:

$$\begin{aligned} \mathbf{H} &= \bar{\mathbf{H}}\Psi \\ &= \bar{\mathbf{Q}} \begin{bmatrix} \bar{r}_{1,1} & 0 & \bar{r}_{1,3} & 0 \\ 0 & \bar{r}_{2,2} & 0 & \bar{r}_{2,4} \\ 0 & 0 & \bar{r}_{3,3} & 0 \\ 0 & 0 & 0 & \bar{r}_{4,4} \end{bmatrix} \begin{bmatrix} c & s & 0 & 0 \\ -s & c & 0 & 0 \\ 0 & 0 & c & s \\ 0 & 0 & -s & c \end{bmatrix} \\ &= \bar{\mathbf{Q}}\mathbf{G}, \end{aligned} \tag{17}$$

where

$$\begin{aligned} \mathbf{G} &= \begin{bmatrix} \mathbf{X} & \mathbf{Y} \\ \mathbf{0} & \mathbf{Z} \end{bmatrix}, \\ \mathbf{X} &= \begin{bmatrix} c\bar{r}_{1,1} & s\bar{r}_{1,1} \\ -s\bar{r}_{2,2} & c\bar{r}_{2,2} \end{bmatrix}, \\ \mathbf{Y} &= \begin{bmatrix} c\bar{r}_{1,3} & s\bar{r}_{1,3} \\ -s\bar{r}_{2,4} & c\bar{r}_{2,4} \end{bmatrix}, \\ \mathbf{Z} &= \begin{bmatrix} c\bar{r}_{3,3} & s\bar{r}_{3,3} \\ -s\bar{r}_{4,4} & c\bar{r}_{4,4} \end{bmatrix}. \end{aligned} \tag{18}$$

Observe that the submatrices $\mathbf{X}$ and $\mathbf{Z}$ are entirely real, since c and s and $\bar{r}_{ii}$, $i \in \{1,2,3,4\}$, are all real. Therefore, we can transform $\mathbf{G}$ into an upper triangular matrix $\mathbf{R} = \mathbf{WG}$ via the purely real Givens rotation matrix:

$$\mathbf{W} = \begin{bmatrix} \mathbf{W}_1 & \mathbf{0} \\ \mathbf{0} & \mathbf{W}_2 \end{bmatrix} \tag{19}$$

where

$$\begin{aligned} \mathbf{W}_1 &= \frac{1}{\sqrt{(c\bar{r}_{1,1})^2 + (s\bar{r}_{2,2})^2}} \begin{bmatrix} c\bar{r}_{1,1} & -s\bar{r}_{2,2} \\ s\bar{r}_{2,2} & c\bar{r}_{1,1} \end{bmatrix}, \\ \mathbf{W}_2 &= \frac{1}{\sqrt{(c\bar{r}_{3,3})^2 + (s\bar{r}_{4,4})^2}} \begin{bmatrix} c\bar{r}_{3,3} & -s\bar{r}_{4,4} \\ s\bar{r}_{4,4} & c\bar{r}_{3,3} \end{bmatrix}. \end{aligned} \tag{20}$$

Substituting $\mathbf{G} = \mathbf{W}^\top\mathbf{R}$ into (17) yields the desired QR decomposition $\mathbf{H} = \mathbf{QR}$, where $\mathbf{Q} = \bar{\mathbf{Q}}\mathbf{W}^\top$ and

$$\mathbf{R} = \mathbf{WG} = \begin{bmatrix} \mathbf{W}_1 & \mathbf{0} \\ \mathbf{0} & \mathbf{W}_2 \end{bmatrix} \begin{bmatrix} \mathbf{X} & \mathbf{Y} \\ \mathbf{0} & \mathbf{Z} \end{bmatrix} = \begin{bmatrix} \mathbf{A} & \mathbf{B} \\ \mathbf{0} & \mathbf{D} \end{bmatrix}. \tag{21}$$

Since $\mathbf{W}_1$, $\mathbf{W}_2$, $\mathbf{X}$ and $\mathbf{Z}$ are all real, it follows that both $\mathbf{A} = \mathbf{W}_1\mathbf{X}$ and $\mathbf{D} = \mathbf{W}_2\mathbf{Z}$ are real. And by construction of $\mathbf{W}_1$ and $\mathbf{W}_2$, both $\mathbf{A}$ and $\mathbf{D}$ are upper triangular.

References

[1] S. M. Alamouti, “A simple transmit diversity technique for wireless communications," *IEEE J. Sel. Areas Commun.*, vol. 16, pp. 1451-1458, Oct. 1998.

[2] V. Tarokh, N. Seshadri, and A. R. Calderbank, “Space-time codes for high data rate wireless communication: performance criterion and code construction," *IEEE Trans. Inf. Theory*, vol. 44, pp. 744-765, Mar. 1998.

[3] J.-C. Belfiore, G. Rekaya, and E. Viterbo, “The golden code: a 2×2 full rate space-time code with non vanishing determinants," *IEEE Trans. Inf. Theory*, vol. 51, no. 4, Apr. 2005.

[4] P. Dayal and M. K. Varanasi, “An optimal two transmit antenna space-time code and its stacked extensions," *IEEE Trans. Inf. Theory*, vol. 51, pp. 4348-4355, Dec. 2005.

[5] L. Zheng and D. Tse, “Diversity and multiplexing: a fundamental tradeoff in multiple antenna channels," *IEEE Trans. Inf. Theory*, vol. 49, no 4, pp. 1073-1096, May 2003.

[6] H. Yao and G. W. Wornell, “Achieving the full MIMO diversity-multiplexing frontier with rotation-based space-time codes," in *Proc. Allerton Conf. Commun., Cont., Computing*, Illinois, Oct. 2003.

[7] IEEE 802.16e-2005: IEEE Standard for Local and Metropolitan Area Networks - Part 16: Air Interface for Fixed and Mobile Broadband Wireless Access Systems - Amendment 2: Physical Layer and Medium Access Control Layers for Combined Fixed and Mobile Operation in Licensed Bands, Feb. 2006.

[8] B. Cerato, G. Masera, and E. Viterbo, “A VLSI decoder for the golden code," 13th *IEEE International Conf. Electronics, Circuits Systems*, ICECS ’06, pp. 549-552, Dec. 2006.

[9] J. Paredes, A. B. Gershman, and M. G. Alkhanari, “A new full-rate full-diversity space-time block code with nonvanishing determinant and simplified maximum-likelihood decoding," *IEEE Trans. Signal Process.*, vol. 56, pp. 2461-2469, June 2008.

[10] S. Sezginer and H. Sari, “Full-rate full-diversity 2×2 space-time codes for reduced decoding complexity," *IEEE Commun. Lett.*, vol. 11, no. 12, pp. 1-3, Dec. 2007.

[11] E. Biglieri, Y. Hong, and E. Viterbo, “On fast decodable space-time block codes," *IEEE Trans. Inf. Theory*, vol. 55, no. 2, pp. 524-530, Feb. 2009.

[12] B. Muquet, S. Sezginer, and H. Sari, “MIMO techniques in mobile WiMAX systems—present and future," *WiMAX Trends*, July 2007.

[13] S. D. Howard, S. Sirianunpiboon, and A. R. Calderbank, “Fast decoding of the golden code by diophantine approximation," in *Proc. IEEE Inf. Theory Workshop*, Lake Tahoe, CA, pp. 590-594, Sep. 2007.

[14] L. Zhang, B. Li, T. Yuan, X. Zhang, and D. Yang, “Golden code with low complexity sphere decoder," in *Proc. 18th Annual IEEE International Symp. Personal, Indoor Mobile Radio Commun. (PIMRC’07)*, pp. 1-5, Athens, Sep. 2007.

[15] M. Sarkiss, J.-C. Belfiore, and Y.-W. Yi, “Performance comparison of different golden code detectors," in *Proc. 18th Annual IEEE International Symp. Personal, Indoor Mobile Radio Commun. (PIMRC’07)*, pp. 1-5, Athens, Sep. 2007.

[16] S. Sirianunpiboon, A. R. Calderbank, and S. D. Howard, “Fast essentially maximum likelihood decoding of the golden code," submitted to *IEEE Trans. Inf. Theory*, 2008.

[17] O. Tirkkonen and R. Kashaev, “Combined information and performance optimization of linear MIMO modulations," in *Proc IEEE Int. Symp. Inf. Theory (ISIT 2002)*, Lausanne, Switzerland, p. 76, June 2002.

[18] A. Wiesel, X. Mestre, A. Pages, and J. R. Fonollosa, “Efficient implementation of sphere demodulation," in *Proc. 4th IEEE Workshop Signal Processing Advances Wireless Commun. (SPAWC 03)*, Rome, Italy, pp. 36-40, June 2003.